Tikrit Journal of Engineering Sciences (2023) 30 (3): 90-99

DOI: http://doi.org/10.25130/tjes.30.3.10

IRAQI Academic Scientific Journals

College of Engineering

ISSN: 1813-162X (Print); 2312-7589 (Online)

Tikrit Journal of Engineering Sciences

available online at: http://www.tj-es.com

TJES Tikrit Journal of Engineering Sciences

Removal of Methylene Blue Dye from Aqueous Solutions Using Cordia Myxa Fruits as a Low-Cost Adsorbent

*Ahmed K. Ibrahim [a], Salwa H. Ahmed [a] *, Riedh A. Abduljabbar [b]*

a Environmental Engineering Department, College of Engineering, Tikrit University, Tikrit, Iraq.

b Department of Biology, College of Science, Tikrit University, Tikrit, Iraq.

Keywords:

Adsorption; Biochar; Carbonization; Cordia Myxa; Methylene Blue Dye.

ARTICLE INFO

Article history:

Received	07 Jan.	2023
Received in revised form	24 June	2023
Accepted	20 June	2023
Final Proofreading	18 Aug.	2023
Available online	06 Sep.	2023

Citation: Ibrahim AK, Ahmed SH, Abduljabbar RA. **Removal of Methylene Blue Dye from Aqueous Solutions Using Cordia Myxa Fruits as a Low-Cost Adsorbent**. *Tikrit Journal of Engineering Sciences* 2023; **30**(3): 90-99.
http://doi.org/10.25130/tjes.30.3.10

Corresponding author:

Salwa H. Ahmed

Environmental Engineering Department, College of Engineering, Tikrit University, Tikrit, Iraq.

Abstract: The dyes make water harmful to humans, animals, and plants and cannot be used until treated. To treat the dyes, non-conventional methods are required, one of which is adsorption with activated carbon. This study aims to produce activated carbon from Cordia myxa fruit (CM) as a low-cost adsorbent to remove methylene blue dye (MB) from aqueous solutions. The characterization of the fabricated-activated carbon was carried out by Brunauer-Emmett-Teller (BET), Fourier-transformed infrared (FTIR), scanning electron microscope (SEM), and X-ray diffraction (XRD) analyses. Different parameters, such as pH (3-9), biochar dose (0.5-5)g/L, initial dye concentration (2-25 mg/L), temperature (25°C), and contact time (0-100 minutes), were examined in batch adsorption experiments. The results showed that the MB dye had a maximum removal efficiency of 68% at a pH of 8, a biochar dosage of 2 g/L, a dye concentration of 30 mg/L, and an 80-minute contact time. The experimental data were analyzed using the Freundlich and Langmuir isotherm models, and their compatibility with the Langmuir isotherm model (R^2=0.9989) was excellent. The study of adsorption kinetics used pseudo-first-order, pseudo-second-order, and Elovich models. The results indicated that the pseudo-second-order was the best model to describe adsorption, with R^2 and K_2 values of 0.99 and 0.0397 g/mg. min, respectively. The negative change in Gibbs free energy (G°) showed spontaneous interaction.

إزالة صبغة الميثيلين الزرقاء من المحاليل المائية باستخدام ثمار البمبر كمادة مازة واطئة الكلفة

احمد خليل ابراهيم [1]، سلوى هادي احمد[1]، رياض عباس عبدالجبار [2]
[1] قسم هندسة البيئة / كلية الهندسة / جامعة تكريت / تكريت – العراق.
[2] قسم علوم الحياة / كلية العلوم / جامعة تكريت / تكريت - العراق.

الخلاصة

تتسبب الصبغات في أن يكون الماء ضارًا بالإنسان والحيوان والنبات ولا يمكن استخدامه إلا بعد معالجته. لمعالجة الأصباغ، يجب استخدام طرق غير تقليدية، منها الامتزاز بالكربون المنشط. باعتبارها مادة ماصة منخفضة التكلفة لإزالة صبغة الميثيلين الزرقاء (MB) من المحاليل المائية، تهدف هذه الدراسة إلى إنتاج الكربون المنشط من ثمار البمبر (CM). تم إجراء توصيف الكربون المنشط بواسطة Brunauer-Emmett-Teller (BET)، تحويل الأشعة تحت الحمراء (FTIR)، مجهر المسح الإلكتروني (SEM)، وتحليلات حيود الأشعة السينية (XRD). تم فحص معلمات مختلفة، مثل الأس الهيدروجيني (3- 9)، جرعة الفحم الحيوي (0.5-5) غم / لتر، تركيز الصبغة الأولي (2-25 مجم / لتر)، درجة الحرارة (25 درجة مئوية)، ووقت التلامس (0-100 دقيقة) في تجارب الامتزاز الدفعي. أظهرت النتائج أن صبغة MB لها كفاءة إزالة قصوى تبلغ 68٪ عند درجة حموضة 8، جرعة فحم حيوي 2 غم / لتر، تركيز صبغة 30 ملغم / لتر، ووقت تلامس 80 دقيقة. تم تحليل البيانات التجريبية باستخدام نموذجي Freundlich وLangmuir متساوي الحرارة، وكان توافقهما مع نموذج Langmuir متساوي الحرارة (R^2 = 0.9989) ممتاز. استخدمت دراسة حركيات الامتزاز نماذج من الدرجة الأولى الزائفة، ومن الدرجة الثانية الزائفة، ونماذج Elovich. أشارت النتائج إلى أن الدرجة الثانية الزائفة هي أفضل نموذج لوصف الامتزاز، حيث بلغت قيم R^2, K^2(0.99، 0.0397 غم / ملغم / دقيقة) على التوالي. يظهر التغيير السلبي في طاقة جيبس الحرة (G^o) أن التفاعل كان تلقائيًا.

الكلمات الدالة: الامتزاز، الفحم الحيوي، الكربنة، البمبر، صبغة المثيلين الزرقاء.

1.INTRODUCTION

Environmental pollution and its problems are among the vital issues that have occupied the world since the beginning of the twentieth century [1]. Industrial, agricultural, and population growth led to using water for utilitarian purposes free from various pollutants, which is constantly decreasing [2]. It is known that various industrial wastes, whether in petrochemical industries or the manufacture of agricultural pesticides, dyes, and other industries, contain slow-decomposing organic compounds that cannot be removed by traditional methods [3-6]. Dyes are considered dangerous industrial pollutants due to the difficulty of their decomposition and their danger to human health, so it has become necessary to find methods to remove these pollutants [7]. Methylene blue (MB) dye has a molecular formula of $C_{16}H_{18}ClN_3S$, a molecular weight of 319.8 g/mol, and its maximum light absorption occurs around 638 nm [8]. MB is a heterocyclic aromatic compound. It is utilized in the textile, paper, and leather industries [9, 10]. Even very low levels of Methylene blue dye in the water can significantly impact aquatic life and the food chain [10]. The MB dye exhibits significant resistance to oxidation by various degradation methods due to its complex aromatic structure [9, 10]. Adsorption is the most widely used method for highly efficient dye removal, and some of its benefits include ease of use, low price, and repeatedly recoverable for future use [11-14]. Many studies deal with removing dyes from aqueous solutions by adsorption on biochar and other adsorbent. Obey et al. [15] used biochar derived from non-customized matamba fruit shells as an adsorbent for wastewater treatment. In their study, adsorption kinetics were performed to assess the adsorption. Elovich was the best model to fit the adsorption kinetics; consequently, the biochar in this study can serve as a promising green material for efficiently removing organic and inorganic contaminants from the environmental water ecosystem. The results indicated that the Matamba fruit shells could be used as an eco-friendly, low-cost, effective adsorbent for anionic dye removal from the water environment. This work intends to manufacture activated carbon from Cordia myxa fruits as an eco-friendly, affordable, and easily available product by recycling fruit waste. The influence of pH, temperature, contact time, and adsorbent dose on the removal efficiency of MB dye from aqueous solution was investigated.

2.MATERIALS AND METHODS

2.1.Materials

2.1.1.Methylene Blue Dye (MB)

The used MB dye (3,7-bis(dimethylamino)) was purchased from the Alhikma market. It is Dark green crystals or crystal-line powder with bronze luster, odorless, stable in air, deep blue solution in water or alcohol, forms double salts, melting point of 100–110 °C (decomposition), density of 1.0 g/mL at 20 °C, and solubility of 43.6 g/L in water at 25 °C.

2.1.2. Producing Activated Carbon from Cordia Myxa Fruit (CM)

After harvesting the Cordia myxa fruit (CM) from the field, it was thoroughly washed with deionized water and dried in the open air for no less than 15 days and no more than 25 days. Then it was thoroughly crushed and sieved using a 425 µm (100 mesh) sieve [16, 17]. The powder was put in a tubular carbonization furnace (saftherm type, China) at a temperature of 600°C for two hours, using nitrogen as an inert gas at a flow rate of 100 ml/min [18]. The tubular furnace was

programmed to gradually increase the temperature at a rate of 5°C/minute until it reached 600°C within 90 minutes. The temperature was fixed at 600 °C for two hours, then gradually decreased for 90 minutes until it reached room temperature. Then the product was taken out of the furnace. The resultant carbon was impregnated in 0.5 M of HCl using a ratio of 1:3 for 24 hours to remove impurities, tar, and cellulose. The final product was washed with distilled water until the pH of the liquid equaled 6.5 [19, 20]. The product was dried in an electric oven at 105°C for 2 hours. The dried product was activated by 0.5 M HCl to produce CM-A adsorbent. Then it was kept in a dark box.

2.2.Characterization of Prepared Activated Carbon (CM-A)

The Brunauer-Emmett-Teller (BET) surface area of CM-A was calculated from N_2 adsorption-desorption isotherms at 77 K using a surface area analyzer (surface area analyzer, BELSORP, Microtrac Co. Japan). The total pore volume (VT), defined as the volume of liquid nitrogen corresponding to the amount adsorbed at a relative pressure of P/P_o= 0.99, was also calculated [19]. The surface functional groups of CM-A were analyzed by Fourier-Transform Infrared Spectroscopy (FTIR). The FTIR spectra of CM-A were analyzed with a Shimadzu 1800 FTIR spectrometer (Shimadzu, Japan). The sample was ground, mixed with KBr, compressed into a thin transparent disk with a diameter of 1 cm, and placed in the FTIR instrument. The spectra were obtained from the pellet with a resolution of 4cm^{-1} at 32 scans min^{-1} and expressed as transmittance in the 400-4000 cm^{-1} range [20, 21]. The morphology of CM-A was observed with a scanning electron microscope (SEM) (JSM-6060 LV, USA). The XRD instrument (Philips PW1730, Netherlands) was employed for CM-A analyses with Cu Kα radiation (λ=1.54A°). The samples were scanned from 5° to 80° (2θ) with a step size of 0.025 and account time of 1 sec at each point.

2.3.Batch Adsorption Experiments

The adsorption experiments were conducted in 100ml conical flasks in a shaking water bath at 150 rpm. The stock solution was prepared with distilled water. The pH was adjusted with 0.1M HCl and 0.1M NaOH. All experiments were conducted in triplicates, and the average values were reported. The optimum pH was calculated by taking 6 samples of pH solutions 3, 5, 6, 7, 8, and 9 with a fixed concentration of the adsorbate (MB) and a fixed dose of the CM-A (activated carbon), where the adsorbate concentration was 5 mg/L, and the dose was 2 g/L. As for the pH values, the alkaline and acidic pH of the solution was maintained by adding amounts of HCl or NaOH solutions at a concentration of 0.1 mol/L at a mixing speed of 150 rpm. The removal efficiency of MB (Eq. 1) was calculated by taking a test for each sample every 10 minutes using a UV-VIS spectrophotometer (Single Beam, Spectro UV-2550, Norway) until it reached equilibrium concentration, the optimum pH, which caused the maximum removal efficiency. The optimum dose of CM-A was calculated by fixing the optimum pH and the concentration of adsorbate and changing the dose of CM-A for six samples 0.5, 1, 2, 3, 4, and 5g/L at a mixing speed of 150 rpm for 80 minutes. From calculating the removal efficiency of MB for each dose, the relationship between dose and removal efficiency was plotted, from which the optimal dose was determined. The effect of the initial concentration of MB dye was carried out by changing the initial concentrations of MB dye from 1 to 40 mg/L while fixing the optimum pH values and dose of CM-A. An optimum dose of CM-A was added to six samples of 100 ml conical flasks of 1, 5, 10, 20, 30, and 40 mg/L MB solution. After each 10-minute, the results from the reaction mixture were analyzed for the rest of MB by taking a sample of 3-4 ml using a syringe and then placing it in a filter paper with a size of 42µm to segregate the activated carbon from the solution and take approximately 1 ml of solution. They placed it in a cuvette in a spectrophotometer, and then the dye concentration was measured using a UV-VIS spectrophotometer with a wavelength of 638 nm. The removal efficiency and amount of dye adsorbed onto CM-A at equilibrium were calculated using Eqs. (1) and (2).

$$R\% = (C_o - C_e) \times 100/C_o \quad \textbf{(1)}$$

where R= Removal efficiency, C_o (mg/L) = Initial concentration, and C_e (mg/L) = effluent equilibrium concentration of MB.

$$q_e = (C_o - C_o) \times V/M \quad \textbf{(2)}$$

where q_e (mg/g)= adsorption capacity, M (g)=dosage of CM-A, and V (L)= Volume of solution.

2.3.1.Adsorption Isotherms

The adsorption isotherms were fitted using Langmuir and Freundlich isotherm models. The Langmuir model is presented in Eq. (3).

$$q_e = K_L \times q_{max} \times C_e/(1 + K_L \times C_e) \quad \textbf{(3)}$$

where q_e(mg/g)= adsorption capacity, K_L(L/mg)= Langmuir's isotherm constant, and q_{max} (mg/g)= maximum adsorption capacity. The Freundlich isotherm model is represented in Eq. (4).

$$\log q_e = 1/n \log C_e + \log k_f \quad \textbf{(4)}$$

where k_f $(mg/g)(L/mg)^{1/n}$= Freundlich adsorption capacity parameter, and 1/n= Freundlich adsorption intensity parameter, unit less.

2.3.2.The Adsorption Kinetic Models

The Adsorption Kinetic Models were described by the pseudo-first-order, pseudo-second-order, and Elovich models. The pseudo-first-order kinetic model assumes that the rate of change of solute absorbance with time is directly

proportional to the difference between the amount of solute adsorbed at the time of equilibrium qe [mg/g] and the amount of solute adsorbed at any time, q(t) (mg/g) [22]. The following is a representation of the Pseudo-first-order velocity expression depending on the adsorbent's capacity Eq. (5) [23]:

$$\ln(q_e - q_t) = \ln q_e - K_1 t \quad \textbf{(5)}$$

where K_1 (min^{-1})= kinetic equilibrium rate constant, q_t (mg/g)= the amounts of adsorbed per unit mass at any time t, and t (min)= contact time. The Pseudo-second-order kinetic model is based on the absorption capacity of the solid phase. Unlike the other model, the concentration predicts behavior over the entire range, which can be called a second-order kinetic velocity equation and can be written as follow Eq. (6) [23]:

$$t/qt = 1/(K_2 \times q_e^2) + t/q_e \quad \textbf{(6)}$$

where K_2 (mg/g.min)= kinetic equilibrium rate constant.

While the Elovich kinetic model assumes that the actual solid surfaces are energetically heterogeneous and that neither desorption nor interactions between the adsorbed species could substantially affect the adsorption kinetics at low surface coverage, it is well-known to describe chemisorption [24]. The Elovich equation is illustrated in Eq. (7).

$$q_t = \beta \ln(\alpha\beta) + \beta \ln t \quad \textbf{(7)}$$

where α (g/mg. min^2)= initial adsorption rate, and β (mg/g.min)= desorption coefficient, equals the activation energy of chemisorption.

2.3.3.Adsorption Thermodynamic

The thermodynamic parameters represented by the change in enthalpy (ΔH°), change in entropy (ΔS°), and change in Gibbs free energy (ΔG°) were calculated using Eqs. (8) – (10).

$$KL = q_e/C_e \quad \textbf{(8)}$$

$$\ln(KL) = \Delta S/R - \Delta H/TR \quad \textbf{(9)}$$

$$\Delta G° = \Delta H° - T\Delta S° \quad \textbf{(10)}$$

where KL (L/g)= the equilibrium thermodynamic constant, R(J/mol. K)= the universal gas constant (= 8.314), T (Kelvin)= the temperature of solution, ΔH°(J/mol)= the change in enthalpy , ΔS°(J/mol. K)= the change in entropy, and ΔG°(J/mol)= the change in Gibbs free energy.

3. RESULTS AND DISCUSSION

3.1.Characterization of Prepared Activated Carbon (CM-A)

The N_2 adsorption and desorption isotherms obtained corresponded to type I, thereby suggesting the presence of micropores [25] (Fig. 1). The Barrett-Joyner-Halenda (BJH) method was used to obtain the pore size distribution curve. The average pore diameter of CM-A was found to be 1.785 nm. Its specific surface area was 1069 ± 1.71 m^2/g with a total pore volume of 0.493 cm^3/g, which indicates that the activated carbon prepared from Cordia myxa fruit had a relatively large surface area and total pore volume compared to commercially available activated carbons such as F100 and BPL from Calgon Corp with BET surface area of 957 and 972 m^2/g and total pore volume of 0.426 and 0.425 cm^3/g, respectively [26].

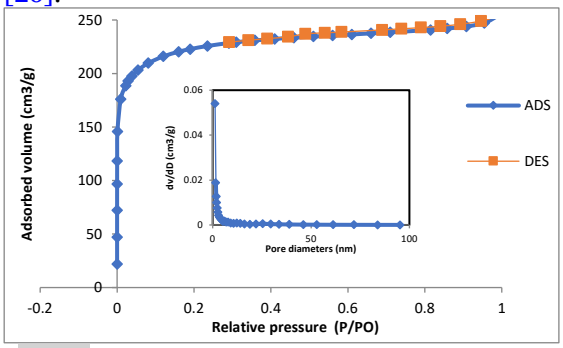

Fig. 1 N_2 Adsorption Isotherm and Pore Size Distribution (Insert) of CM-A.

The results of examining the FTIR spectra on the sample of the adsorbent used in this study are shown in Fig. 2. It is noted that the sample was devoid of organic compounds except for the carbonyl group C=O in Quinone, which caused clear peaks of the beam at 1529.6 cm^{-1} [27]. It showed the characteristics of CM-A at 2879.8 and 2999.4 cm^{-1} as C-H stretching on methylene and C-H stretching on methyl, respectively [28]. It is also noted that the sample that represented the adsorbent contains more groups of the inorganic compounds at the wavenumbers less than 600 cm^{-1} [29], where the peaks at the wavenumber of 530.4 and 493.7 cm^{-1}, while the peak at 705 cm^{-1} was attributed to aromatic C-H stretching that appeared on the CM-A surface [30]; however, the beams greater than 3000 cm^{-1} explains the OH group presence in the sample, i.e., moisture, that may be caused from the air while handling the sample and before or during the examination, as in the wavenumber range of 3410.2 to 3531.78 cm^{-1}[31]. These results are consistent with those obtained by [32].

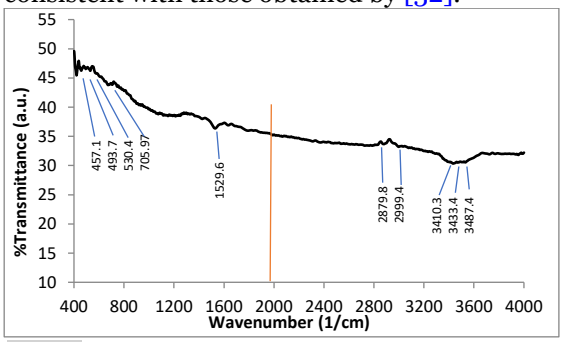

Fig. 2 FTIR Spectra of the Produced Activated Carbon CM-A.

The morphology of CM-A was investigated using SEM in Fig. 3 (a, b). Fig.3 shows the cross-sectional view of CM-A with x70 and x135 magnification, respectively. The CM-A SEM explains the porosity development of the prepared activated carbons after activation and

carbonization at the optimum operating conditions. It is noted that the external surface contained few pores. Furthermore, SEM showed different porosities dispersed at different distances. The porosity also depends on the raw material type [23].

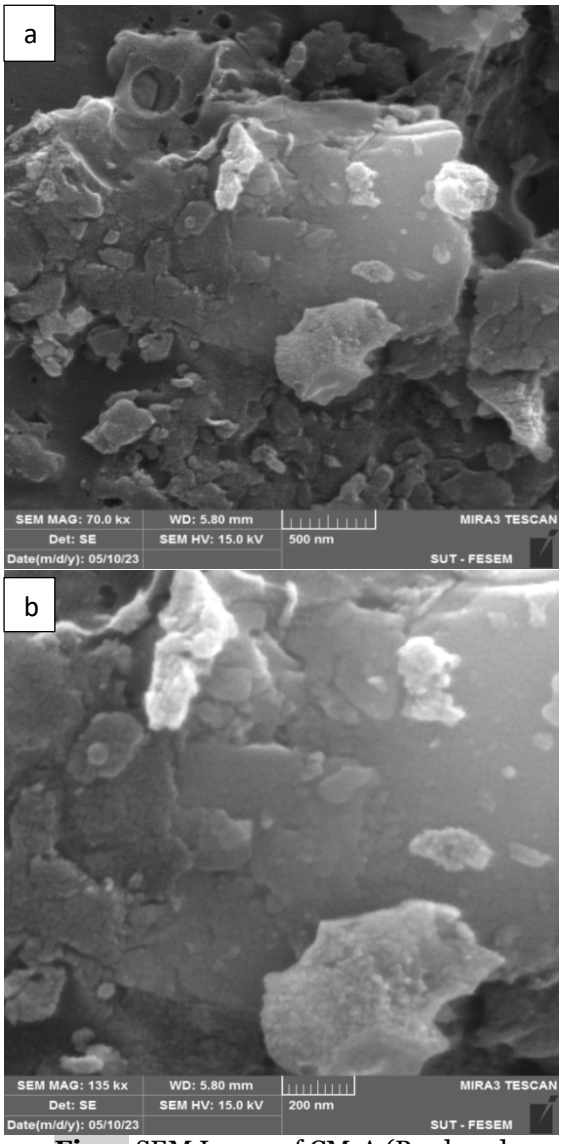

Fig. 3 SEM Image of CM-A (Produced Activated Carbon) at (a) x70 Magnification and (b) x135 Magnification.

The XRD result of CM-A is shown in Fig. 4. The diffraction patterns agree well with the standard JCPDS file (41–1487), which confirmed the formation of crystalline structures of the graphitic carbon. The peaks of 2 theta (2θ) at 26.014°, 42.134°, and 45.211° are indexed to the corresponding peaks for (002), (100), and (101) crystal planes of graphitic carbon, respectively. The sharp peak around 26° confirmed the crystalline structure of CM-A, which portrayed the superior alignment of disordered graphitic carbon layers to form the crystalline turbostratic structure [33]. From the FWHM value of the highly intense peak, the average crystallite size of CM-A was calculated corresponding to the (002) crystal plane, and it was 1.37 nm. Because of the carbon transition from a high symmetric phase to a lower one, the peak splitting was observed in the X-ray diffraction peaks. It also showed the microporous wall structure of CM-A presence.

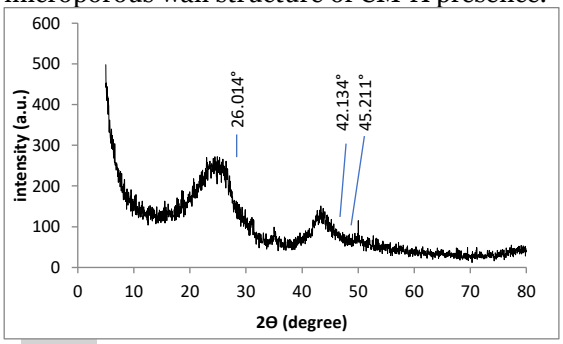

Fig. 4 XRD Analyses Result Obtained From CM-A Adsorbent.

3.2.Effect of pH on Removal Efficiency of MB Dye

The relationship between the contact time and the dye removal efficiency (calculated from Eq. (1)) for solutions with different pH values showed an increase in the removal efficiency with the contact time, however, with varying values depending on the pH values. The maximum removal efficiency was approximately 68% at the contact time of 80 minutes and pH=8. While the minimum removal efficiency at pH=3 was about 20% at the same contact time, which was attributed to hydrogen ions competing with the dye on the adsorption site [34] (Fig. 5). Parallel results are possible to see in different literature [35, 36].

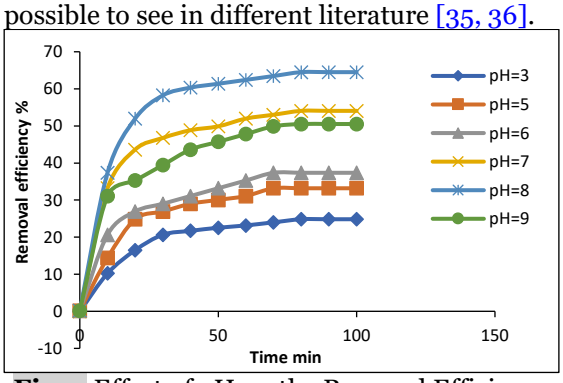

Fig. 5 Effect of pH on the Removal Efficiency of MB Dye Onto CM-A (MB Dye Conc. of 5mg/L, Temperature of 25°C, and CM-A Dose of 2 g/L).

3.3.Effect of Adsorbent Dosage on Removal Efficiency

The results showed that the optimal dose of CM-A was 2 g/L. In the case of decreasing the dose, the removal efficiency of MB dye decreased due to the dye competing on adsorption locations [37]. When increasing the dose to more than 2 g/L, the dye removal efficiency increased due to the different charge attractions on the surfaces of both the dye and the adsorbent [38]. As there was no drastic increase in the adsorption rate on increasing the dosage of adsorbent beyond 2 g/L of CM-A,

hence, from an economic point of view, 2 g/L was considered the optimum dosage for the removal of methylene blue [38], as shown in Fig. 6.

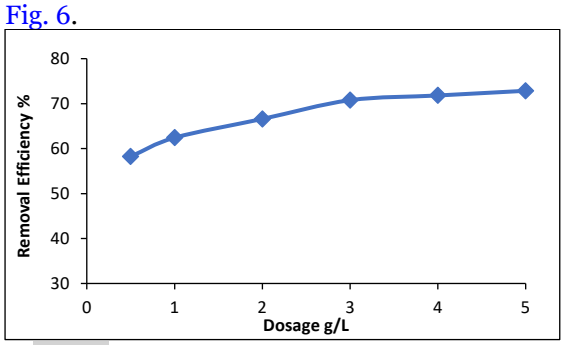

Fig. 6 Effect of Dose of CM-A on Removal Efficiency of MB Dye (MB Dye Conc. of 5mg/L, Temperature of 25°C, and pH=8).

3.4. Effect of Initial Concentration of MB Dye on Removal Efficiency

The relationship between the initial concentration of MB and the removal efficiency is shown in Fig. 7. As the removal efficiency increased with the dye's initial concentration until it reached the maximum value of 68% at a concentration of MB of 30 mg/L, which attributed to the fact that the mass transfer driving force would become more significant on the initial concentration increasing, resulting in higher adsorption of MB [39]. Then the efficiency gradually decreased with the continued increase in the dye's initial concentration because of competition on locations of adsorption [37, 40]. Similar observations were reported by the adsorption of MB on activated carbons prepared from jute fiber [41], olive-seed waste residue [42], and corncob [43].

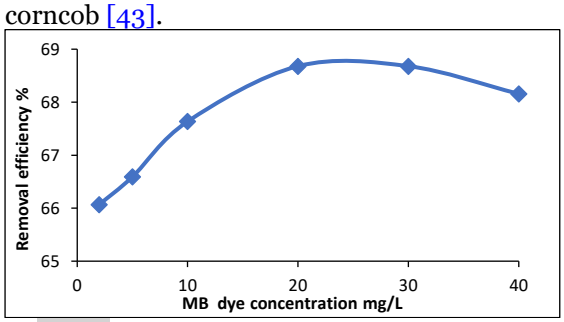

Fig. 7 Effect of MB Dye Concentration on Removal Efficiency by CM-A. (CM-A Dose of 2g/L, Temperature of 25°C, and pH=8).

3.5. Adsorption Isotherms

The Langmuir and Freundlich isothermal models were used to understand adsorption to remove a specific pollutant from aqueous solutions using a specific adsorbent material.

3.5.1.Langmuir Isotherm Model

The best straight line that can be drawn is the line with a correlation coefficient value very close to 1. From the equation of this line, the maximum MB adsorption capacity (q_{max}) of CM-A and Langmuir constant (K_L) were 71.43 and 0.029, respectively, as shown in Fig. 8 and Table 1.

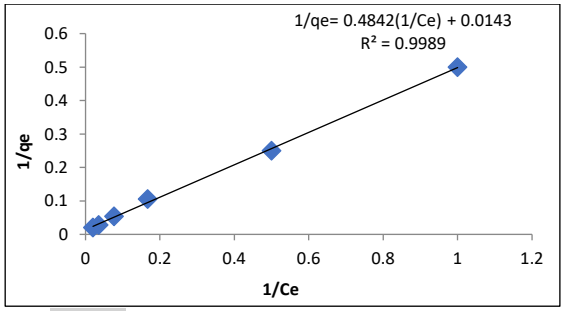

Fig. 8 Langmuir Model to Examine the Adsorption Behavior of MB Dye onto CM-A.

3.5.2.Freundlich Isotherm Model

A straight line passing through the largest number of points drawn depending on the values of log(Ce) vs. log(qe) resulted in the values of 1/n, Kf, and R^2 to be 0.828, 0.139, and 0.997, respectively, where the value 1/n indicates that the adsorption is favorable because it was between 0 and 1. As for the value of R^2, it was very close to 1 (Fig. 9), indicating that the straight line passes through the largest number of points, as in Table 1.

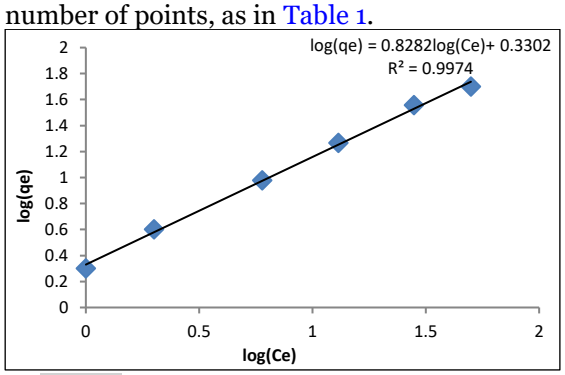

Fig. 9 Freundlich Model to Examine the Adsorption Behavior of MB Dye onto CM-A.

The results showed that the Langmuir model was suitable for demonstrating the adsorption of MB onto CM-A, as in Table 1. These results are very close to what the researchers reached in [44, 45].

Table 1 Isotherm Parameters for the MB by CM-A Removal.

Model	Langmuir	Freundlich
Isotherm parameter	q_{max}= 71.43 mg/g	1/n=0.8282
	1/ ($K_L.q_{max}$)=0.4842 g/L	kf=2.139
	K_L=0 .0295 L/mg	(mg/g)(L/mg)$^{1/n}$
	*R^2=0.9989	R^2=0.997

*R^2=1- (sum of squared differences between model and experiment/ sum of squared differences between experiment and average)

3.6.Kinetic Study

The appropriate kinetic model is when the graph line passes through all the points. The results showed that the pseudo-second-order was the best model to describe the experimental data, i.e., the value of K_2=0.0397 g/mg. min and R^2=0.999. (Fig. 10 (a, b, c)). These results are similar to the findings of the two researchers [16, 46, 47].

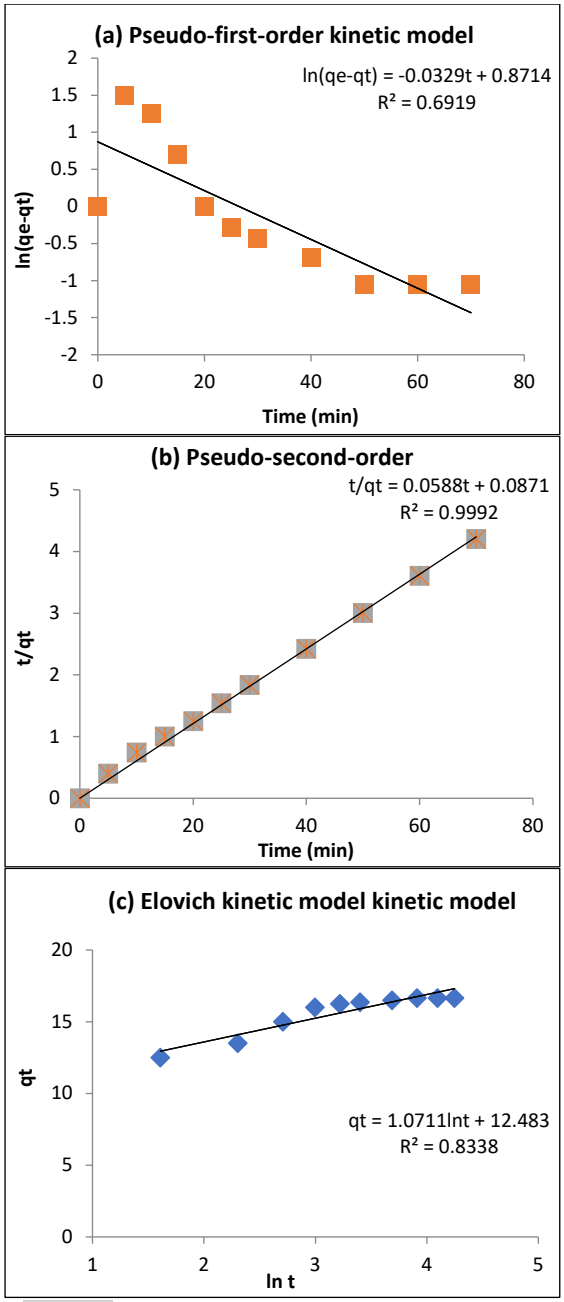

Fig. 10 (a) Pseudo-First-Order, (b) Pseudo-Second-Order, (c) Elovich Models to Examine the Adsorption Behavior of Cm-A for MB Dye.

3.7. Adsorption Thermodynamics

The thermodynamic parameters represented by the change in enthalpy (ΔH°), change in entropy (ΔS°), and change in Gibbs free energy (ΔG°) were calculated using a sample of a solution containing MB at a concentration of 100 mg/L, the adsorbent dose was 2 g/L of activated carbon, the pH was 8, the mixing speed was 150 rpm and at a temperature of 25° C until the solution reached its equilibrium state. The q_e was calculated after finding C_e using a UV-VIS spectrophotometer from Eq. (2), while K_L was calculated using Eq. (8). The work above was repeated in the same conditions except for a change in the temperature at 35 °C and 45 °C from drawing the relationship between 1/T and ln(K_L), Eq. (9), to obtain ΔH and ΔS, and obtain ΔG form Eq. (10) at temperatures of 25, 35, and 45°C at optimum values of pH, adsorbent dose, and adsorbate concentration. A positive value of ΔG° indicates that the reaction was not spontaneous and vice versa.

The ΔH° value was +5.56 KJ/mol indicating that the adsorption interaction was endothermic (positive value), while the values of ΔG° at 25 °C, 35 °C, and 45 °C were negative values indicating that the adsorption interaction was spontaneous; however, the ΔS° value was +18.9 J/mol.K indicating a certain structural modification and decrease the system regularity in the solid/liquid interface (Table 2). The above results are close to previous studies [48, 49].

Table 2 Thermodynamic Parameter for MB Dye Adsorption onto CM-A

Temperature (°C)	Temperature (K)	K_L	ΔG° (KJ/mol)	ΔH° (KJ/mol)	ΔS° (J./mol.K)	R^2
25	298	1.02	-0.067			
35	308	1.14	-0.354	5.556	18.9	0.908
45	318	1.18	-0.442			

The negative value of Gibb's free energy showed the thermodynamic feasibility and spontaneity of the sorption process; however, the enthalpy (ΔH°) positive value confirmed that the adsorption was endothermic in nature and increased with temperature [18], while the entropy (ΔS°) positive value indicated the randomness decreased at the solid-solution interface during the fixation of absorbates on the adsorbent active sites [37].

4. CONCLUSION

The Methylene Blue Dye adsorption from aqueous solutions was performed using the adsorbent CM Fruits. The results confirmed that CM is a promising adsorbent material because it is eco-friendly, available, and low-cost for treating contaminated dye wastewater at ambient temperatures. The adsorption efficiency strongly depended on the adsorbent dose, contact time, and initial dye concentration. The highest removal efficiency of 68% was obtained at 2 g of CM, 80 min, and 30 mg/L, respectively. The results indicated that the Langmuir model showed a better fit to the experimental data because the multi-layer adsorption happened, which agrees with the applicability of the Langmuir isotherm model. The adsorption rate was found to fit pseudo-second-order kinetics with a high correlation coefficient (R^2= 0.999) for all studied concentrations. Thus, it can be concluded that CM-A can be used as a cost-effective alternative material for MB dye removal in wastewater treatment processes.

REFERENCES

[1] Boisvenue C, Running SW. **Impacts of Climate Change on Natural Forest Productivity–Evidence Since The Middle of The 20th Century**. *Global Change Biology* 2006;**12**:(862–882).

[2] Bogardi JJ, Leentvaar J, Sebesvári Z. Biologia Futura: **Integrating Freshwater Ecosystem Health in Water Resources Management**. *Biologia Futura* 2020;**71**:(337–358).

[3] Ibrahim A. **Effect of The Horizontal Perforated Plates on The Turbidity Removal Efficiency in Water Treatment Plant of Tikrit University**. *Tikrit Journal of Engineering Sciences* 2019;**26**:(38–42).

[4] Rasheed, T., Shafi, S., Bilal, M., Hussain, T., Sher, F., & Rizwan, K. **Surfactants-Based Remediation as an Effective Approach for Removal of Environmental Pollutants—A Review**. *Journal of Molecular Liquids* 2020;**318**:(113960).

[5] Ahmed SH, Ibrahim AK, Abed MF. **Assessing the Quality of the Groundwater and the Nitrate Exposure, North Salah Al-Din Governorate, Iraq: Quality of Groundwater**. *Tikrit Journal of Engineering Sciences* 2023;**30**:(25–36).

[6] Ibrahim AK. **Improvement of removal efficiency of water supply plant by using polyelectrolyte type LT-22 with alum**. *Materials Today: Proceedings* 2021;**42**:(1928–1933).

[7] Lin Y-TT, Kao FY, Chen SH, Wey M-YY, Tseng HH. **A Facile Approach From Waste to Resource: Reclaimed Rubber-Derived Membrane for Dye Removal**. *Journal of the Taiwan Institute of Chemical Engineers* 2020;**112**:(286–295).

[8] Miclescu A, Wiklund L. **Methylene Blue, an Old Drug with New Indications**. *Jurnalal Roman de Anestezie Terapie Intensiva* 2010;**17**:(35–41).

[9] Abbas M, Trari M. **Removal of Methylene Blue In Aqueous Solution by Economic Adsorbent Derived from Apricot Stone Activated Carbon**. *Fibers and Polymers* 2020;**21**:(810–820).

[10] Moorthy AK, Rathi BG, Shukla SP, Kumar K, Bharti VS. **Acute Toxicity of Textile Dye Methylene Blue on Growth and Metabolism of Selected Freshwater Microalgae.** *Environmental Toxicology and Pharmacology* 2021;**82**:(103552).

[11] Meng L, Zhang X, Tang Y, Su K, Kong J. **Hierarchically Porous Silicon–Carbon–Nitrogen Hybrid Materials Towards Highly Efficient and Selective Adsorption Of Organic Dyes**. *Scientific Reports* 2015;**5**:(1–16).

[12] Diao H, Zhang Z, Liu Y, Song Z, Zhou L, Duan Y., and Zhang J. **Facile Fabrication of Carboxylated Cellulose Nanocrystal–Mno2 Beads for High-Efficiency Removal Of Methylene Blue**. *Cellulose* 2020;**27**:(7053–7066).

[13] Huang, Y., Ho, S. S. H., Lu, Y., Niu, R., Xu, L., Cao, J., & Lee, S. **Removal of Indoor Volatile Organic Compounds via Photocatalytic Oxidation: A Short Review and Prospect**. *Molecules* 2016;**21**:56, (1-20).

[14] Seidensticker S, Zarfl C, Cirpka OA, Fellenberg G, Grathwohl P. **Shift in Mass Transfer of Wastewater Contaminants from Microplastics in The Presence of Dissolved Substances**. *Environmental Science & Technology* 2017;**51**:(12254–12263).

[15] Obey G, Adelaide M, Ramaraj R. **Biochar Derived from Non-Customized Matamba Fruit Shell as an Adsorbent for Wastewater Treatment**. *Journal of Bioresources and Bioproducts* 2022;**7**:(109–115).

[16] Mashkoor F, Nasar A. **Magsorbents: Potential Candidates in Wastewater Treatment Technology–A Review on The Removal of Methylene Blue Dye**. *Journal of Magnetism and Magnetic Materials* 2020;**500**:(166408).

[17] Wanyonyi WC, Onyari JM, Shiundu PM. **Adsorption of Congo Red Dye from Aqueous Solutions Using Roots of Eichhornia Crassipes: Kinetic and Equilibrium Studies**. *Energy Procedia* 2014;**50**:(862–869).

[18] Morin M, Pécate S, Masi E, Hémati M. Kinetic Study and Modelling of Char Combustion in TGA in Isothermal Conditions. *Fuel* 2017;**203**:(522–536).

[19] Junior, O. P., Cazetta, A. L., Gomes, R. C., Barizão, É. O., Souza, I. P., Martins,

A. C., Asefa, T., & Almeida, V. C. **Synthesis of ZnCl2-activated Carbon from Macadamia Nut Endocarp (Macadamia Integrifolia) by Microwave-Assisted Pyrolysis: Optimization Using RSM and Methylene Blue Adsorption**. *Journal of Analytical and Applied Pyrolysis* 2014;**105**:(166–176).

[20] Bayati, M., Numaan, M., Kadhem, A., Salahshoor, Z., Qasim, S., Deng, H., & de Cortalezzi, M. F. **Adsorption of Atrazine by Laser Induced Graphitic Material: An Efficient, Scalable and Green Alternative for Pollution Abatement**. *Journal of Environmental Chemical Engineering* 2020;**8**(5):(104-107).

[21] Jung, M. R., Horgen, F. D., Orski, S. V., Rodriguez, V., Beers, K. L., Balazs, G. H., Jones, T. Todd, & Lynch, J. M. **Validation of ATR FT-IR to Identify Polymers of Plastic Marine Debris, Including Those Ingested by Marine Organisms**. *Marine Pollution Bulletin* 2018;**127**:(704–716).

[22] Revellame ED, Fortela DL, Sharp W, Hernandez R, Zappi ME. **Adsorption Kinetic Modeling Using Pseudo-First Order and Pseudo-Second Order Rate Laws: A Review**. *Cleaner Engineering and Technology* 2020;**1**:100032, (1-13).

[23] Kılıç M, Janabi ASK. **Investigation of Dyes Adsorption with Activated Carbon Obtained from Cordia myxa**. *Bilge International Journal of Science and Technology Research* 2017;**1**:(87–104).

[24] Song S, Li B. **Adsorption At Natural Minerals/Water Interfaces**. Springer; 2021.

[25] Qian D, Lei C, Wang E, Li W, Lu A. **A Method for Creating Microporous Carbon Materials with Excellent CO2 - Adsorption Capacity and Selectivity**. *ChemSusChem* 2014;**7**:(291–298).

[26] Yuan X, Shi X, Zeng S, Wei Y. **Activated Carbons Prepared from Biogas Residue: Characterization and Methylene Blue Adsorption Capacity.** *Journal of Chemical Technology & Biotechnology* 2011;**86**:(361–366).

[27] Zhang Y, Xu X, Zhang P, Zhao L, Qiu H, Cao X. **Pyrolysis-Temperature Depended Quinone and Carbonyl Groups as The Electron Accepting Sites in Barley Grass Derived Biochar.** *Chemosphere* 2019;**232**:(273–280).

[28] Sun S, Wang A. **Adsorption Kinetics of Cu(II) Ions Using N,O-Carboxymethyl-Chitosan.** *Journal of Hazardous Materials* 2006;131:(103–111).

[29] Amine Fersi M, Chaabane I, Gargouri M, Bulou A. **A Theoretical Study on The Molecular Structure of New Organic–Inorganic Bis-(4-Acetylanilinium) Tetrachloridozincate Compound.** *Indian Journal of Physics* 2016;**90**:381–389.

[30] Zhao B, Nartey OD. **Characterization and Evaluation of Biochars Derived from Agricultural Waste Biomasses from Gansu, China**. *Proceedings of the World Congress on Advances in Civil, Environmental, and Materials Research, Busan, Republic of Korea,* 2014; **30**:1-17.

[31] Khurshid, H., Mustafa, M. R. U., Rashid, U., Isa, M. H., Ho, Y. C., & Shah, M. M. **Adsorptive Removal of COD from Produced Water Using Tea Waste Biochar**. *Environmental Technology & Innovation* 2021;**23**:(101563).

[32] Pundir A, Garg M, Singh R. **Evaluation of Properties of Gypsum Plaster-Superplasticizer Blends of Improved Performance.** *Journal of Building Engineering* 2015;**4**:(223–230).

[33] Kalagatur, N. K., Karthick, K., Allen, J. A., Nirmal Ghosh, O. S., Chandranayaka, S., Gupta, V. K., & Mudili, V. **Application of Activated Carbon Derived from Seed Shells of Jatropha curcas for Decontamination of Zearalenone Mycotoxin.** *Frontiers in Pharmacology* 2017; **8**. (760-770).

[34] Foo KY, Hameed BH. **An Overview of Dye Removal via Activated Carbon Adsorption Process.** *Desalination and Water Treatment* 2010;**19**:(255–274).

[35] Ezeonuegbu, B. A., Machido, D. A., Whong, C. M., Japhet, W. S., Alexiou, A., Elazab, S. T., ... & Batiha, G. E. S.. **Agricultural Waste of Sugarcane Bagasse as Efficient Adsorbent for Lead and Nickel Removal from Untreated Wastewater:**

Biosorption, Equilibrium Isotherms, Kinetics and Desorption Studies. *Biotechnology Reports* 2021;**30**:e00614, (1-10).

[36] Theng ML, Tan LS. **Optimization on Methylene Blue and Congo Red Dye Adsorption onto Cassava Leaf using Response Surface Methodology.** *Malaysian Journal of Catalysis* 2020;**4:**(34–38).

[37] Calimli MH, Nas MS, Burhan H, Mustafov SD, Demirbas Ö, & Sen, F. **Preparation, Characterization and Adsorption Kinetics of Methylene Blue Dye n Reduced-Graphene Oxide Supported Nanoadsorbents.** *Journal of Molecular Liquids* 2020;**309**:(113171).

[38] Zhu Z, Wu P, Liu G, He X, Qi B, Zeng G, & Cui, F. **Ultrahigh Adsorption Capacity of Anionic Dyes With Sharp Selectivity Through The Cationic Charged Hybrid Nanofibrous Membranes.** *Chemical Engineering Journal* 2017;**313**:(957–966).

[39] Tan IAW, Ahmad AL, Hameed BH. **Adsorption of Basic Dye on High-Surface-Area Activated Carbon Prepared From Coconut Husk: Equilibrium, Kinetic and Thermodynamic Studies.** *Journal of Hazardous Materials* 2008;**154**:(337–346).

[40] Ahmed SH. **Cu II Removal from Industrial Wastewater Using Low Cost Adsorbent.** *Tikrit Journal of Engineering Sciences* 2017;**24**:(44–50).

[41] Senthilkumaar S, Varadarajan PR, Porkodi K, Subbhuraam C V. **Adsorption of Methylene Blue onto Jute Fiber Carbon: Kinetics and Equilibrium Studies.** *Journal of Colloid and Interface Science* 2005;**284**:(78–82).

[42] Stavropoulos GG, Zabaniotou AA. **Production and Characterization of Activated Carbons from Olive-Seed Waste Residue.** *Microporous and Mesoporous Materials* 2005;**82**:(79–85).

[43] El-Sayed GO, Yehia MM, Asaad AA. **Assessment of Activated Carbon Prepared from Corncob by Chemical Activation with Phosphoric Acid.** *Water Resources and Industry* 2014;**7**:(66–75).

[44] Zhu N, Yan T, Qiao J, Cao H. **Adsorption of Arsenic, Phosphorus and Chromium by Bismuth Impregnated Biochar: Adsorption Mechanism and Depleted Adsorbent Utilization**. *Chemosphere* 2016;**164**:(32–40).

[45] Belhaj AF, Elraies KA, Alnarabiji MS, Kareem FAA, Shuhli JA, Mahmood, S. M., & Belhaj, H. **Experimental Investigation, Binary Modelling and Artificial Neural Network Prediction of Surfactant Adsorption for Enhanced Oil Recovery Application.** *Chemical Engineering Journal* 2021;**406**:127081. (1-15).

[46] Demirbaş Ö, Çalımlı MH, Demirkan B, Alma MH, Nas MS, Khan A, Abdullah M. Asiri, & Şen, F.. **Thermodynamics, Kinetics, and Adsorption Properties of Biomolecules onto Carbon-Based Materials Obtained from Food Wastes.** *BioNanoScience* 2019;**9**:(672–682).

[47] Nas MS, Calimli MH, Burhan H, Yılmaz M, Mustafov SD, Sen F. **Synthesis, Characterization, Kinetics and Adsorption Properties of Pt-Co@ GO Nano-Adsorbent for Methylene Blue Removal in The Aquatic Mediums Using Ultrasonic Process Systems.** *Journal of Molecular Liquids* 2019;**296**:(112100).

[48] NAS MS. **The Investigation of Thermodynamics Parameters and Adsorption Kinetic of The Maxilon Blue 5G Dye on Turkey Green Clay.** *Journal of the Institute of Science and Technology* 2019;**9**:(749–758).

[49] Cheng J, Zhan C, Wu J, Cui Z, Si J, Wang Q, Peng X, & Turng L. **Highly Efficient Removal of Methylene Blue Dye from an Aqueous Solution Using Cellulose Acetate Nanofibrous Membranes Modified by Polydopamine.** *ACS Omega* 2020;**5**:(5389–5400).